

Fill in the Gap! Combining Self-supervised Representation Learning with Neural Audio Synthesis for Speech Inpainting

Ihab Asaad, Maxime Jacquelin, Olivier Perrotin, Laurent Girin, Thomas Hueber

Abstract—Most speech self-supervised learning (SSL) models are trained with a pretext task which consists in predicting missing parts of the input signal, either future segments (causal prediction) or segments masked anywhere within the input (non-causal prediction). Learned speech representations can then be efficiently transferred to downstream tasks (e.g., automatic speech or speaker recognition). In the present study, we investigate the use of a speech SSL model for *speech inpainting*, that is reconstructing a missing portion of a speech signal from its surrounding context, i.e., fulfilling a downstream task that is very similar to the pretext task. To that purpose, we combine an SSL encoder, namely HuBERT, with a neural vocoder, namely HiFiGAN, playing the role of a decoder. In particular, we propose two solutions to match the HuBERT output with the HiFiGAN input, by freezing one and fine-tuning the other, and vice versa. Performance of both approaches was assessed in single- and multi-speaker settings, for both informed and blind inpainting configurations (i.e., the position of the mask is known or unknown, respectively), with different objective metrics and a perceptual evaluation. Performances show that if both solutions allow to correctly reconstruct signal portions up to the size of 200 ms (and even 400 ms in some cases), fine-tuning the SSL encoder provides a more accurate signal reconstruction in the single-speaker setting case, while freezing it (and training the neural vocoder instead) is a better strategy when dealing with multi-speaker data.

Index Terms—Speech inpainting, self supervised model, speech synthesis, speech enhancement, neural vocoder.

I. INTRODUCTION

SPEECH and/or audio inpainting aims at enhancing speech and/or audio signals that are “locally” degraded. Focusing initially on short gaps (i.e., a few milliseconds), the first targeted applications were packet loss recovery in telecommunications and streaming audio [1] or signal declipping [2]. More recent studies addressed longer gaps between 50 ms and up to 400 ms, e.g. [3], [4], [5], [6]. Early works were based on signal processing techniques, such as linear predictive coding [7], sinusoidal modelling [3], or graphs [8]. Recently, speech/audio inpainting has been tackled with deep neural networks (DNNs), mostly with fully-supervised learning and encoder-decoder architectures, the encoder being fed with the

Ihab Asaad and Maxime Jacquelin contributed equally to this work. Ihab Asaad worked on this project during his stay at Univ. Grenoble Alpes. He is now with the Friedrich Schiller Universität Jena, Jena, Germany (e-mail: ihab.asaad@uni-jena.de). Maxime Jacquelin, Olivier Perrotin, Laurent Girin and Thomas Hueber are with Univ. Grenoble Alpes, CNRS, Grenoble-INP, Grenoble, France (e-mails: firstname.name@grenoble-inp.fr).

This work was supported in part by MIAI @ Grenoble Alpes (ANR-19-P3IA-0003) and by ANRT CIFRE. Submitted for review on 2024-05-23.

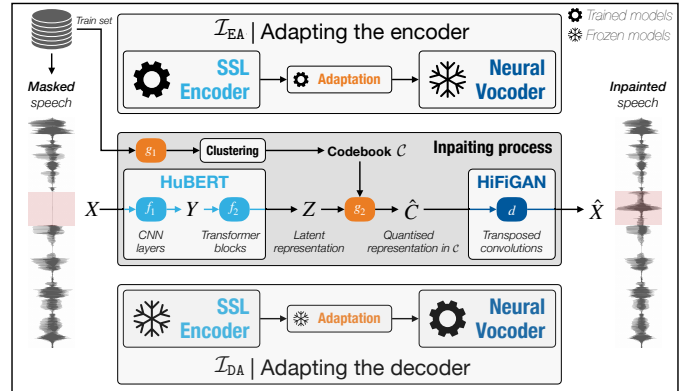


Fig. 1. Proposed inpainting frameworks combining a self-supervised learning model and a neural vocoder. Top: The SSL encoder is fine-tuned while the neural vocoder is kept frozen. Bottom: The SSL encoder is kept frozen while the neural vocoder is trained. In the present study we use HuBERT as the SSL and HiFiGAN as the vocoder (subfigure in the middle). The inpainting process and adaptation mechanism between the SSL output and neural vocoder input are detailed in Sec. II).

signal surrounding the gap and the decoder being in charge of generating the signal within the gap. Music signals with gaps above 64 ms were processed in [9] with an encoder based on a convolutional neural network (CNN), and in [4] with one based on a generative adversarial network (GAN). In [5], a U-net architecture was trained to inpaint the magnitude spectrogram of speech signals with gaps in both the time or frequency dimensions. Moreover, a VGG-like feature extractor [10], pre-trained on a word classification task, was used based on the assumption that it would improve the linguistic content of the inpainted spectrogram. This work was recently extended in [6] by adding an additional adversarial loss. A few studies also investigated the use of a visual input such as the speaker’s lips for guiding the speech inpainting process, implemented with an LSTM- or Transformer-based context encoder [4], [11]. It can be noted that all these studies work in the time-frequency (TF) domain, inpainting the magnitude spectrogram of speech/audio signals. The inpainted magnitude spectrogram must then be combined with a phase reconstruction algorithm, e.g. [12], [13], before applying inverse TF transform to obtain the inpainted time-domain waveform.

All the above-mentioned deep-learning-based inpainting studies are based on supervised learning, basically a mapping between the incomplete signal and the complete one. Interestingly, speech inpainting is implicitly at the core of (speech)

self-supervised (representation) learning (SSL) [14], in which deep neural networks are trained to learn an efficient speech signal representation via the prediction of signal parts that are artificially made missing –a process referred to as *masking* in this framework. The prediction can be causal (exploiting past and present context to predict the future signal) as in, e.g., autoregressive predictive coding (APC) [15] and contrastive predictive coding (CPC) [16], or non-causal (exploiting both past and future contexts to predict a missing part anywhere in the signal), as in Transformer-based SSL models such as HuBERT [17], wav2vec [18], or WavLM [19]. By exploiting regularities at multiple time scales, and therefore multiple linguistic levels (i.e., from phonetics to semantics) [20], such models encode rich representations of the speech signal that can be efficiently transferred to a variety of downstream tasks, including automatic speech, speaker, or emotion recognition [21]. In fact, the SSL models have been used and evaluated exclusively on these downstream tasks, which happen to be classification tasks, and have become very popular because of the impressive performance they have shown there. To the best of our knowledge –and quite surprisingly– SSL models have not been used for inpainting nor evaluated on this task, even though, as already mentioned, “unmasking” is the central *pretext task* of SSL models training. In this study, we investigate the ability of a non-causal SSL model, in the present case HuBERT, to “fill in the gap” by reconstructing the missing part of a speech signal from its surrounding context.

Since HuBERT does not directly predict the missing time-domain signal samples but rather high-dimensional embeddings, a specific algorithm is needed to go back to the time-domain signal. Neural vocoders such as WaveNet [22] or HiFiGAN [23] have shown to be more efficient than phase reconstruction algorithms, at least for speech. We thus propose to combine an SSL encoder (here HuBERT) with a neural vocoder (in the present case HiFiGAN) for speech inpainting. We propose two ways to do that, either by training the neural vocoder on the pre-trained SSL output, or by fine-tuning the pre-trained SSL on the neural vocoder input. The first approach is inspired by the low-bitrate neural speech coding approach proposed in [24]. The second one involves to fine-tune HuBERT to predict directly a Mel-scaled magnitude spectrogram for the masked part, which is the standard input of a vanilla HiFiGAN. The two proposed frameworks are illustrated in Fig. 1. We assess the performance of these two methods in both single-speaker and more challenging multi-speaker settings, with both objective metrics and perceptual tests. Importantly, we provide the complete source code, pre-trained models and demo pages, for the two proposed inpainting frameworks.¹

II. METHOD

A. Problem formulation

Following the notations used in [14], let us denote $X = \{x_1, \dots, x_T\}$ a sequence of speech samples of length T (i.e., a waveform), and $X_{-[t_1, t_2]}$ the sequence in which the segment $X_{t \in [t_1, t_2]} = \{x_{t_1}, x_{t_1+1}, \dots, x_{t_2}\}$ is masked, i.e. replaced

with zeros. In the following of this paper, we will address *non-causal* inpainting, i.e., the inpainting function \mathcal{I} has access to past and future unmasked parts of the input signal. We will consider both the *informed* inpainting paradigm, i.e. when the mask position is known, and the *blind* one, i.e. when the mask position is not known. The informed inpainting process consists in predicting the missing segment from its surrounding context while keeping the original signal on the unmasked parts, i.e. $\hat{X}_{t \in [t_1, t_2]} = \mathcal{I}(X_{-[t_1, t_2]})$ and $\hat{X}_{t \notin [t_1, t_2]} = X_{t \notin [t_1, t_2]}$. In blind inpainting, the entire output signal is generated without differentiating the masked and unmasked parts, i.e. $\hat{X} = \mathcal{I}(X_{-[t_1, t_2]})$.

B. Masking, the core pretext task of HuBERT

HuBERT is an encoder that converts an audio signal X to a latent representation $Z = \{z_1, \dots, z_L\}$ of size L [17]:²

$$\begin{aligned} y_l &= f_1(X_{[lH-u, lH+u]}), \\ Z &= f_2(Y), \text{ with } Y = \{y_1, \dots, y_L\}, \end{aligned} \quad (1)$$

where f_1 , sometimes referred to as the prenet, is a stack of CNNs of span $2u$ samples and hop size H , and f_2 is a stack of Transformer encoder blocks. During training, part of the CNN-encoded sequence Y is randomly masked to predict the fully-encoded sequence Z , i.e., Y is replaced by $Y_{-[l_1, l_2]}$ in (2), which amounts to masking the corresponding samples in X . HuBERT is iteratively trained to predict a vector-quantised representation of the speech signal, denoted C (e.g., vector-quantised Mel-frequency cepstral coefficient (MFCC) vectors in the first vanilla HuBERT training iteration). This is done with the help of two auxiliary modules, g_1 and g_2 , which act as teacher and student models, respectively. The teacher module g_1 maps the audio signal to the new representation (unquantised MFCC vectors in the above example), with a span of $2w$ samples and window shift H . Before training, a codebook \mathcal{C} of quantised prototype vectors is obtained by passing part of the training set through g_1 and applying a k-means algorithm on the output. During training, g_1 and vector quantisation (VQ) are applied to extract a ‘reference’ quantised sequence $C = \{c_1, \dots, c_L\}$ from each waveform of the train dataset:

$$c_l = \text{VQ}_{\mathcal{C}}(g_1(X_{[lH-w, lH+w]})), \quad (3)$$

where $\text{VQ}_{\mathcal{C}}$ stands for VQ using the codebook \mathcal{C} . The student module g_2 aims at predicting this quantised sequence from the encoder output Z :

$$\hat{c}_l = g_2(z_l) = g_2 \circ f_2 \circ f_1(X_{[lH-u, lH+u]}). \quad (4)$$

The predicted sequence $\hat{C} = \{\hat{c}_1, \dots, \hat{c}_L\}$ is expected to be as close as possible to the reference sequence C . In practice, g_2 is implemented with a softmax function involving a (learned) linear projection of z_l over \hat{c}_l . During HuBERT training, g_1 is fixed, and f_1 , f_2 and g_2 are updated to minimise the distance between \hat{C} and C while part of the Y sequence is randomly

²In the following equations, when chaining several functions, we do not differentiate if a function applies to a vector of a sequence (at frame l) or to the complete sequence. This abuse of notation is to notably simplify the presentation, without affecting the principle of the proposed methodology.

¹<https://gricad-gitlab.univ-grenoble-alpes.fr/huebert/speech-inpainting>

masked across batches. Note that g_1 and g_2 are only used for HuBERT pre-training, and are generally discarded at inference time when using HuBERT in a downstream task. The pre-trained HuBERT is thus composed of $f_2 \circ f_1$ only, and a newly trained module dedicated to the downstream task is generally appended to f_2 .

To the best of our knowledge, in the many different uses of HuBERT reported in the literature, the masking is only used for training and is never kept during inference. In other words, when using the speech representation Z in downstream tasks, the input signal X is generally *not* masked. However, we hypothesise that at inference, HuBERT should be able to encode a masked input $X_{-[t_1, t_2]}$, since this is equivalent to masking part of the Y sequence in the pretext training task. In other words, HuBERT is implicitly an inpainting encoder, even if, to our knowledge, it has not been considered as such in the literature.

We showed that during training on masked signals, HuBERT performs inpainting with a quantised representation of the input signal (see (4)). Therefore, to carefully match the pretext training task when performing inpainting in inference, we keep the auxiliary module g_2 responsible for the quantisation of Z . We then obtain a complete inpainting framework by first encoding a masked waveform:

$$\hat{C} = g_2 \circ f_2 \circ f_1 (X_{-[t_1, t_2]}) \quad (5)$$

and, with the addition of a decoder d , then convert the inpainted quantised sequence \hat{C} to a waveform \hat{X} . In the informed case, this writes:

$$\begin{cases} \hat{X}_{t \in [t_1, t_2]} &= d(\hat{C}_{l \in [l_1, l_2]}) \\ \hat{X}_{t \notin [t_1, t_2]} &= X_{t \notin [t_1, t_2]}, \end{cases} \quad (6)$$

where $[l_1, l_2]$ is the frame interval corresponding to the masked sample interval $[t_1, t_2]$. For the blind case, we simply have:

$$\hat{X} = d(\hat{C}). \quad (7)$$

In the following, we detail how to adapt g_2 for interfacing HuBERT ($f_2 \circ f_1$) and the decoder (d), and how to accordingly set up g_1 and the codebook \mathcal{C} to train g_2 .

C. Combining HuBERT encoder with HiFiGAN decoder

In this work, we choose HiFiGAN [23] as the decoder, as it showed one of the highest performance in the most recent text-to-speech synthesis benchmark [25] and for its versatility to various input formats [24]. The latter point is crucial in our study since we need to make the encoder output and decoder input compatible. We propose two *frameworks* for this sake: (i) decoder adaptation (DA), in which the HiFiGAN decoder is trained to fit a frozen pre-trained HuBERT, and (ii) encoder adaptation (EA), in which we fine-tune the HuBERT encoder output to fit the standard frozen HiFiGAN decoder. These methods are illustrated in Fig. 1 and detailed below.

1) *Decoder adaptation*: In this first approach, we use a pre-trained HuBERT model and keep it frozen. To adapt the HiFiGAN decoder to the frozen pre-trained HuBERT, we follow the two-step adaptation process used in the GSLM framework [24]. In the first step, we directly use Z as the new

signal representation (i.e., $g_1^{(\text{DA})}$ is identical to the frozen pre-trained HuBERT $f_2 \circ f_1$). A new codebook $\mathcal{C}^{(\text{DA})}$ is obtained by running the k-means algorithm on the Z sequences obtained on part of the pre-training dataset. $g_2^{(\text{DA})}$ is then simply the quantisation on $\mathcal{C}^{(\text{DA})}$ of the encoding Z of any masked input sequence $X_{-[t_1, t_2]}$:

$$\hat{C} = g_2^{(\text{DA})}(Z) = \text{VQ}_{\mathcal{C}^{(\text{DA})}}(f_2 \circ f_1(X_{-[t_1, t_2]})) \quad (8)$$

In the second step, we learn from scratch an adapted version of HiFiGAN $d^{(\text{DA})}$, similar to the one used in [24]. More specifically, the decoder takes the index of each \hat{c}_L in the codebook $\mathcal{C}^{(\text{DA})}$ as input, and learns a look-up table of embedding vectors that feed the vanilla HiFiGAN architecture. By noting with * the modules that are trained, the full inpainting pipeline \mathcal{I}_{DA} is therefore:

$$\hat{X} = \mathcal{I}_{\text{DA}}(X_{-[t_1, t_2]}) = d^{(\text{DA})} * \circ g_2^{(\text{DA})} \circ f_2 \circ f_1(X_{-[t_1, t_2]}). \quad (9)$$

2) *Encoder adaptation*: In this second approach, we use the vanilla HiFiGAN decoder, which uses a Mel-spectrogram as input, and keep it frozen, whereas we adapt HuBERT. To understand well our adaptation of HuBERT and the motivation behind it, we first need to come back to the conventional HuBERT training, which principle was given in Section II-B.

As described in details in [17], after pre-training HuBERT on the masking pretext task with the help of g_1 and g_2 , the model is fine-tuned on an Automatic Speech Recognition (ASR) task. In that case, g_1 and g_2 are discarded, and f_2 is appended with a softmax layer for phoneme class prediction (the ground truth being obtained from a labelled dataset). When fine-tuning f_2 for this task, this ASR-oriented supervised training may encourage the encoder to extract linguistic information, however at the expense of supra-segmental information, such as intonation, which is yet essential to recover in an inpainting task. In our EA solution to inpainting, we aim at benefiting from the powerful pre-trained HuBERT while somehow “cancelling” its fine-tuning on the ASR task, and at the same time at adapting the HuBERT output to the Mel-spectrogram HiFiGAN input representation. This is done by reintroducing g_1 and g_2 , and performing a new iteration of training on a reasonable amount of training data with the masking pretext task, and by using the Mel-spectrum (MS) as the speech representation (hence our adaptation process can be seen as some kind of fine-tuning).

In a few more details, we define $g_1^{(\text{EA})}$ as the extraction of MS vectors from (frames of $2w$ samples of) the waveforms X . The codebook $\mathcal{C}^{(\text{EA})}$ is obtained with the k-means algorithm applied on the output of $g_1^{(\text{EA})}$ for a train set. Given an input sequence X , the teacher module $g_1^{(\text{EA})}$ computes an MS vector for each frame, which is assigned to its closest centroid in $\mathcal{C}^{(\text{EA})}$ (as in (3)). The student softmax-based $g_2^{(\text{EA})}$ module of [17] is also re-introduced, to predict a sequence \hat{C} of quantised MS vectors in $\mathcal{C}^{(\text{EA})}$:

$$\hat{c}_l = g_2^{(\text{EA})}(z_l) = \underset{c}{\operatorname{argmax}} \left(\frac{\exp\left(\frac{\sin(Az_l, e_c^{(\text{EA})})}{\tau}\right)}{\sum_{c'=1}^{\text{Card}(\mathcal{C}^{(\text{EA})})} \exp\left(\frac{\sin(Az_l, e_{c'}^{(\text{EA})})}{\tau}\right)} \right), \quad (10)$$

where A is a linear projection, $\text{sim}(a, b)$ is the cosine similarity between a and b , $e_c^{(\text{EA})}$ is a learnt embedding of codeword $c \in \mathcal{C}^{(\text{EA})}$, and τ is the logit scale factor [17], set to 0.1. Following HuBERT training described in Section II-B, $g_1^{(\text{EA})}$ and f_1 are fixed, and f_2 and $g_2^{(\text{EA})}$ are updated to minimise the cross-entropy loss between the predicted MS vectors \hat{c}_l and the quantised MS vectors $c_l \in \mathcal{C}^{(\text{EA})}$, while part of the Y sequence is randomly masked across batches. At inference, the sequence \hat{C} of quantised MS vectors is directly fed to a pre-trained vanilla HiFiGAN. By noting again by * the modules that are trained, the full \mathcal{I}_{EA} framework is therefore:

$$\hat{X} = \mathcal{I}_{\text{EA}}(X_{-[t_1, t_2]}) = d \circ g_2^{(\text{EA})*} \circ f_2^* \circ f_1(X_{-[t_1, t_2]}). \quad (11)$$

III. EXPERIMENTAL SET-UP

A. Datasets

We conducted experiments on both LJ Speech [26] and VCTK [27] datasets. LJ Speech is an English corpus containing 13 100 short audio clips recorded by a single female speaker for a total length of approximately 24 h. We isolated 12 950 clips as the training/validation set, the remaining 150 clips being used for test. VCTK includes a set of 43 859 audio clips recorded by 109 English speakers balanced in gender and with various accents, for a total of approximately 44 h. We used 41 747 clips from 105 speakers for training and 389 clips from 4 speakers for test. Importantly, we carefully designed the partitioning of the VCTK dataset to have no overlap between the training and test sets in terms of sentences and speakers. In other words, the proposed models have to generalise to both new speakers and new linguistic content.

B. Implementation details

a) SSL encoder HuBERT: For the two proposed inpainting frameworks \mathcal{I}_{DA} and \mathcal{I}_{EA} , we used the HuBERT-large model *hubert-large-ls960-ft*, publicly available on HuggingFace (see our repository). This model is a fine-tuned version of *hubert-large-ll60k*, the latter being initially trained on the Libri-Light dataset [28], including 60 000 h of speech data from over 7000 speakers. The fine-tuning was done on the LibriSpeech dataset, containing 960 h of speech data from over 2484 speakers. To the best of our knowledge, the LJ Speech and VCTK datasets used in the present study are not included in LibriSpeech. However, since LJ Speech is extracted from the LibriVox³ dataset, there might be a slight overlap with the very large Libri-Light dataset (also based on LibriVox). However, this overlap is approximately 0.0004% (24 vs. 60 000 hours) and thus remains very limited.

In the HuBERT model used in this study, the speech input is expected to be sampled at 16 kHz. The prenet window size and hop size are 8960 and 320 samples, respectively. The output Z has dimension 768.

b) Adapting the neural vocoder (\mathcal{I}_{DA}): For this approach, we used the implementation of the speech encoder-decoder framework proposed by [24]. Dedicated codebooks $\mathcal{C}^{(\text{DA})}$ were computed using the LJ Speech (resp. VCTK) dataset, considering a training subset of 21 h (resp. 36 h) and 100 (resp. 500) clusters. Recall that for this model $g_2^{(\text{DA})}$ is not trained, i.e. for any representation Z of a masked input sequence $X_{-[t_1, t_2]}$, $g_2^{(\text{DA})}$ retrieves the closest sequence of vectors $\hat{C} = \{\hat{c}_1, \dots, \hat{c}_L\}$ from $\mathcal{C}^{(\text{DA})}$. HiFiGAN is then trained from scratch to generate \hat{X} from \hat{C} . For the multi-speaker configuration (i.e. model trained and evaluated on the VCTK dataset), a speaker embedding extracted using the speaker identification model proposed in [29] was used as an additional conditioning vector. Here, we trained this model on the same VCTK training subset than for the codebook computation (36 h). Both the HiFiGAN vocoder and the speaker identification model were trained with the Adam optimiser [30] over 200 epochs, with a batch size of 32 and a learning rate of 2×10^{-4} .

c) Adapting the SSL encoder (\mathcal{I}_{EA}): In this second approach, the HuBERT encoder is fine-tuned to directly predict a quantised Mel-spectrogram representation, which is converted back to a time-domain audio signal with HiFiGAN. More precisely, $g_2^{(\text{EA})}$ is an additional linear layer designed to adapt the HuBERT output Z to a quantised Mel-spectrogram domain, as defined in equation 10). The Transformer blocks f_2 are fine-tuned while $g_2^{(\text{EA})}$ is trained from scratch. For this sake, the teacher $g_1^{(\text{EA})}$ computes 80-dimensional MS vectors from the input speech, with a window size of 46 ms and a hop size of 20 ms. Dedicated codebooks $\mathcal{C}^{(\text{EA})}$ were computed on the LJ Speech (resp. VCTK) training subset. As for the \mathcal{I}_{DA} framework, we used 100 (resp. 500) clusters, but with the k-means applied on MS vectors obtained from $g_1^{(\text{EA})}$. For each training set (LJ speech or VCTK), fine-tuning f_2 and training $g_2^{(\text{EA})}$ was done using the Adam optimiser over 100 epochs, with a batch size of 8 and a learning rate of 10^{-4} .

For the audio synthesis, we used a pretrained HiFiGAN model,⁴ taking an 80-dimensional Mel-spectrogram as input, and generating a waveform at 22.05 kHz.⁵ While being optional, a slight fine-tuning of HiFiGAN on quantised ground-truth Mel-spectrograms was found to be beneficial for the overall audio quality. This was done using Adam over 50 epochs, with a batch size of 8 and a learning rate of 10^{-4} .

d) Post-processing: For the blind inpainting case, the reconstructed signal was generated entirely by the neural vocoder. For the informed case, we kept only the generated signal corresponding to the masked part and we placed it within the original (masked) signal using a cross-fade of 5 ms on both sides. Finally, the inpainted signals obtained with the \mathcal{I}_{EA} framework were resampled to 16 kHz for a fair comparison with the other framework and baseline.

⁴More specifically, we used the UNIVERSAL_V1 model (see our repository).

⁵An upsampling of HuBERT's codebook, initially computed considering 16 kHz speech input, was therefore necessary.

³<https://librivox.org>

C. Baselines

As a baseline, we implemented a simple inpainting method based on linear interpolation (\mathcal{I}_{LI}). For a given masked signal, it consists in calculating its Mel-spectrogram (as done in Section III-B) and replacing the masked frames with a linear interpolation between the last frame before the mask and the first frame after the mask. The interpolated Mel-spectrogram was then fed to the pre-trained HiFiGAN vocoder to generate a 22.05 kHz waveform, which was then downsampled to 16 kHz.

We also wanted to compare the proposed speech inpainting frameworks with other recently published methods such as [5] and [6]. Unfortunately, no source code is publicly available for these studies (confirmed by the contacted authors) and we could not perform experiments with these methods with the exact same configurations as the ones used in the proposed frameworks. Nevertheless, since we use common metrics (detailed below), in Sec. IV we compare our results with the ones reported in [5] and [6], at least in terms of order of magnitude.

D. Objective metrics

We evaluated the inpainted speech quality using PESQ [31] and its intelligibility using STOI [32] on both LJ Speech and VCTK test sets, comprising 150 and 389 utterances, respectively. Each utterance was masked three times using mask lengths of 100, 200 and 400 ms, and whose position was randomly chosen in each utterance, resulting in 539×3 masked utterances to inpaint with our three frameworks (\mathcal{I}_{LI} , \mathcal{I}_{DA} , \mathcal{I}_{EA}). PESQ and STOI were computed by considering segments of one second of speech, centred on the mask (therefore, the inpainted speech corresponds to 10, 20, or 40% of the original speech when measuring the score). As a complementary objective evaluation, we also performed automatic speech recognition (ASR) on the inpainted speech. We used a pre-trained Whisper model [33] and report the character error rate (CER).⁶ For all metrics, average scores on each test set and each mask length are reported for all systems, with the binomial proportion confidence interval.

E. Perceptual evaluation

To further investigate the performance of the proposed inpainting system, we conducted an online MUSHRA-based listening test using the Web Audio Evaluation Tool [34]. This was done only for the informed case. First, we randomly sampled 15 sentences from the LJ Speech test set (mono-speaker condition), and 15 sentences from the VCTK test set (multi-speaker condition). For each sentence, we randomly masked a 200 ms-long segment and inpainted it with \mathcal{I}_{EA} , \mathcal{I}_{DA} , and with the \mathcal{I}_{LI} baseline. Finally, we asked 72 native English speakers (self-reported as British or American, recruited via the Prolific platform⁷) to evaluate the quality of the inpainted speech using a MUSHRA-based protocol [35]. For each sentence, presented

in random order, participants had to rate comparatively the three inpainted signals as well as a high-anchor signal (natural speech). The type of each signal (natural or inpainted) was not given to participants. As a reference, participants also received both the original sound file and its textual transcription. To rate the four stimuli, participants were instructed to focus on the inpainted speech segment which was highlighted using square brackets around the corresponding textual transcription. Following the post-screening procedure described in [35], we excluded 28 participants who ranked the hidden natural speech less than 90 out of 100, for more than 15% of the stimuli (resulting in a final set of 44 participants who were considered as performing the test correctly).

F. Statistical analysis

In the following, we assess the effect of the *mask length*, *framework*, *dataset* (mono- vs. multi-speaker) and *type of inpainting* (informed vs. blind) factors, when relevant, on the objective and subjective metrics. We each time use a beta regression model (using the R function `glmTMB`), followed by post-hoc pairwise comparisons between factor levels (R function `glht`). Details of factors involved in each statistical analysis are given in the next Section. Significance level is systematically set to $p < 0.01$.

IV. RESULTS

A. Qualitative results

Examples of inpainted speech signals obtained with the two proposed frameworks (\mathcal{I}_{EA} and \mathcal{I}_{DA}) and with the baseline \mathcal{I}_{LI} , in the informed case, and for a mask length of 200 ms, are presented in Fig. 2. Other examples, for other mask lengths, are available on our demo webpage⁸. We first examine the spectral pattern observed for the linear baseline \mathcal{I}_{LI} . Recall that the Mel-spectrogram is computed from the audio output of the HiFiGAN vocoder, the latter being fed with a linearly interpolated mel-spectrogram between the beginning and the end of the mask. Interestingly, despite this “linear input”, the inpainted speech is almost –but not entirely– stationary. In fact, for the mono-speaker case (left column), we can observe a transient a few milliseconds after the start of the mask. Consequently, the neural vocoder has “shaped” the linear input (likely not seen in its training corpus), probably by exploiting contextual information. However, as our quantitative evaluation confirms (see Sec. IV-B1), this minimal sound shaping is not precise enough to recover the phonetic content of the masked part and the speech inpainted by the \mathcal{I}_{LI} framework is most often not intelligible.

We now qualitatively compare the two proposed inpainting frameworks \mathcal{I}_{EA} and \mathcal{I}_{DA} . For the mono-speaker case (left column), the signal to be reconstructed corresponds to approximately 2 phones: a post-alveolar affricate / tʃ / followed by a vowel / e / (in the word *suggestion*). The complex spectral pattern associated with this phonetic sequence is better reconstructed by the \mathcal{I}_{EA} framework than with \mathcal{I}_{DA} , with a sharper vowel-consonant transition (\mathcal{I}_{DA} wrongly maintains a

⁶This metric provides useful information about the phonetic content of the inpainted speech but may be biased by the linguistic prior on which the ASR may rely to transcribe it.

⁷<https://www.prolific.co>

⁸http://www.ultraspeech.com/demo/iecc_taslp2024_inpainting/

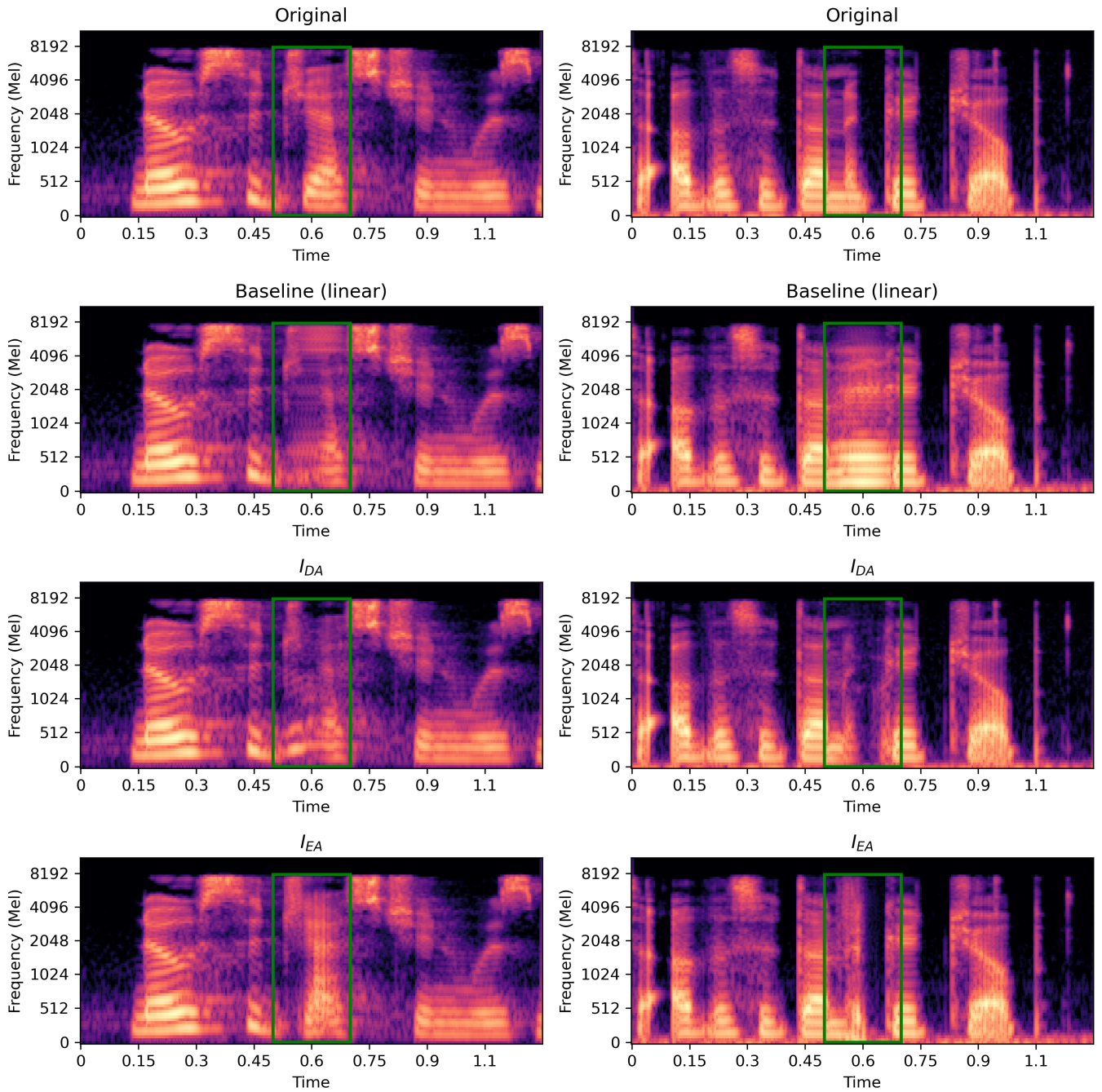


Fig. 2. Examples of inpainted speech signals (80-dimensional Mel-spectrograms, informed case). Left: Mono-speaker for the sentence “no su[gg]est[ion] was made”, Right: Multi-speaker for the sentence “(...) has do[ne] a goo[d] job”. The green rectangles illustrate the position and length of the mask (200 ms).

strong formants structure during the consonant). For the multi-speaker case (right column), the signal to inpaint corresponds to the phonetic sequence [n ə g ʊ]. Here, \mathcal{I}_{EA} is less efficient. It correctly reconstructs the initial nasal n as well as the plosive g and the final vowel ʊ but surprisingly replaces the middle schwa ə with an unvoiced and high energy sound, creating a kind of audio artefact. This is not the case with the \mathcal{I}_{DA} framework, with which the signal is very well reconstructed. These initial qualitative results are confirmed by the quantitative evaluation presented in the following sections.

B. Informed inpainting

1) *Objective evaluation*: The results of the objective evaluation of informed inpainting in terms of PESQ, STOI and CER scores are presented in Table I. We assessed here the significance of *mask length* (100, 200, 400 ms), *framework* (\mathcal{I}_{LI} , \mathcal{I}_{DA} , \mathcal{I}_{EA}) and *dataset* (mono- and multi-speaker) with the test utterances as a random factor for each objective metric. Statistical analysis showed that all factors and all their interactions have a significant effect on each objective metric. Non-significant pairs of distributions shown by post-hoc

TABLE I

INFORMED SPEECH INPAINTING RESULTS. FOR ALL METRICS, AVERAGE SCORES WITH CONFIDENCE INTERVALS FOR EACH TEST SET, EACH MASK LENGTH, AND EACH FRAMEWORK, FOR BOTH THE MONO- AND MULTI-SPEAKER CONFIGURATIONS. THE BEST SCORES PER FRAMEWORK ARE DENOTED IN BOLD. PAIRS OF SYMBOLS INDICATE PAIRS OF DISTRIBUTIONS THAT ARE NOT SIGNIFICANTLY DIFFERENT.

Mono-speaker (LJ Speech)					Multi-speaker (VCTK)		
Models	Mask (ms)	PESQ [-0.5; 4.5] \uparrow	STOI [0; 1] \uparrow	CER (%) \downarrow	PESQ [-0.5; 4.5] \uparrow	STOI [0; 1] \uparrow	CER (%) \downarrow
Unmasked	0	4.25 \pm 0.04	0.97 \pm 0.01	6 \pm 1	4.05 \pm 0.06	0.94 \pm 0.01	4 \pm 2
Baseline \mathcal{I}_{LI}	100	2.92 \pm 0.16	0.92 \pm 0.04	13 \pm 9	2.40 \pm 0.15	0.87 \pm 0.06	17 \pm 7
	200	2.25 \pm 0.17	0.83 \pm 0.06	16 \pm 7	1.97 \pm 0.18	0.77 \pm 0.04	13 \pm 4
	400	1.95 \pm 0.13	0.71 \pm 0.05	19 \pm 5	1.57 \pm 0.16	0.60 \pm 0.05	22 \pm 6
\mathcal{I}_{DA}	100	3.06 \pm 0.17	0.94 \pm 0.04	15 \pm 6 \blacksquare	3.13 \pm 0.08	0.93 \pm 0.01	8 \pm 5
	200	2.85 \pm 0.18	0.89 \pm 0.05 \blacktriangleright	13 \pm 9 \blacksquare \blacklozenge \blacktriangle	2.93 \pm 0.11	0.88 \pm 0.03 \blacktriangleright	15 \pm 7 \blacktriangle
	400	2.78 \pm 0.16	0.86 \pm 0.05 \star	24 \pm 14	2.66 \pm 0.11	0.83 \pm 0.03	18 \pm 7 \bullet
\mathcal{I}_{EA}	100	3.28 \pm 0.07	0.96 \pm 0.03	7 \pm 3	3.06 \pm 0.10	0.90 \pm 0.07	10 \pm 6
	200	3.09 \pm 0.08	0.93 \pm 0.04	12 \pm 5 \blacklozenge \blacktriangledown	2.70 \pm 0.15	0.85 \pm 0.09	12 \pm 5 \blacktriangledown
	400	2.93 \pm 0.13	0.86 \pm 0.06 \star	14 \pm 4	2.39 \pm 0.17	0.79 \pm 0.11	19 \pm 8 \bullet

TABLE II

BLIND SPEECH INPAINTING RESULTS. FOR ALL METRICS, AVERAGE SCORES WITH CONFIDENCE INTERVALS FOR EACH TEST SET, EACH MASK LENGTH, AND EACH FRAMEWORK, FOR BOTH THE MONO- AND MULTI-SPEAKER CONFIGURATIONS. THE BEST SCORES PER FRAMEWORK ARE DENOTED IN BOLD. PAIRS OF SYMBOLS INDICATE PAIRS OF DISTRIBUTIONS THAT ARE NOT SIGNIFICANTLY DIFFERENT.

Mono-speaker (LJ Speech)					Multi-speaker (VCTK)		
Models	Mask (ms)	PESQ [-0.5; 4.5] \uparrow	STOI [0; 1] \uparrow	CER (%) \downarrow	PESQ [-0.5; 4.5] \uparrow	STOI [0; 1] \uparrow	CER (%) \downarrow
\mathcal{I}_{DA}	0	2.87 \pm 0.08	0.89 \pm 0.01	19 \pm 7	3.11 \pm 0.04	0.93 \pm 0.01	13 \pm 5
	100	2.77 \pm 0.17	0.88 \pm 0.03 \blacktriangle	40 \pm 11	2.93 \pm 0.09	0.89 \pm 0.02 \blacktriangle	26 \pm 7
	200	2.33 \pm 0.17 \blacktriangleleft	0.75 \pm 0.05	57 \pm 14	2.31 \pm 0.11 \blacktriangleleft	0.71 \pm 0.03	31 \pm 10
	400	1.72 \pm 0.15	0.54 \pm 0.05 \blacktriangleright	81 \pm 17	1.53 \pm 0.11	0.52 \pm 0.03 \blacklozenge \blacktriangleright	51 \pm 9
\mathcal{I}_{EA}	0	3.46 \pm 0.03	0.95 \pm 0.01	15 \pm 6	2.78 \pm 0.02	0.89 \pm 0.01	16 \pm 4
	100	2.81 \pm 0.15	0.90 \pm 0.05	17 \pm 9	2.57 \pm 0.16	0.81 \pm 0.08	20 \pm 8
	200	2.55 \pm 0.17	0.84 \pm 0.06	24 \pm 14	2.23 \pm 0.13	0.69 \pm 0.10	41 \pm 19
	400	1.97 \pm 0.16	0.79 \pm 0.06	39 \pm 8	1.39 \pm 0.19	0.51 \pm 0.10 \blacklozenge	56 \pm 21

analyses are indicated by pairs of symbols in Table I and reported accordingly in the text.

a) Influence of mask length: Pairwise comparisons show significant differences between the three *mask length* levels, on all metrics, for each *framework* and each *dataset*, except in terms of CER between mask lengths of 100 ms and 200 ms in the $\mathcal{I}_{DA} \times$ mono-speaker condition (\blacksquare). As expected, as the mask length increases from 100 to 400 ms, the performance across all evaluated metrics decreases. For example, for the \mathcal{I}_{EA} framework, the PESQ score is 3.28 for a mask length of 100 ms and it drops to 2.93 for a mask length of 400 ms.

b) Comparison with the baseline: Pairwise differences between the three inpainting *frameworks* metric distributions are significant for all *mask length* and *datasets*, except between the \mathcal{I}_{DA} and \mathcal{I}_{EA} frameworks in terms of STOI in the 400 ms \times Mono-speaker (\star) condition ; and in terms of CER in the 200 ms \times mono-speaker (\blacklozenge) and in the 400 ms \times multi-speaker (\bullet) conditions. In particular, both proposed inpainting frameworks (\mathcal{I}_{EA} and \mathcal{I}_{DA}) obtain scores that are systematically greater (and often much greater) than those obtained by the \mathcal{I}_{LI} baseline, for both the mono-speaker and multi-speaker cases. This confirms the expected need for a non-linear modelling to fill gaps that include more than a diphone transition. This also demonstrates the interest of

using a powerful encoder like HuBERT, which is able to exploit the contextual information to access the high-level linguistic information needed for inpainting long gaps.

c) Mono-speaker vs. multi-speaker: All metrics distributions between *datasets* are also significant for each *framework* and *mask length*, except between the mono- and multi-speaker datasets in terms of STOI in the $\mathcal{I}_{DA} \times$ 200 ms (\blacktriangleright) condition ; and in terms of CER in the $\mathcal{I}_{DA} \times$ 200 ms (\blacktriangle) and in the $\mathcal{I}_{EA} \times$ 200 ms (\blacktriangledown) conditions. Interestingly, results display a strong interaction between the *dataset* and the *framework* factors. In the mono-speaker case, the \mathcal{I}_{EA} framework (fine-tuned SSL encoder) consistently outperforms the \mathcal{I}_{DA} framework (frozen SSL encoder) across all evaluated metrics. For example, for a mask length of 100 ms, \mathcal{I}_{EA} achieves a PESQ score of 3.28, a STOI score of 0.96, and a CER of 7%, whereas \mathcal{I}_{DA} obtains 3.06, 0.94, and 15%, respectively. Conversely, in the multi-speaker setting (VCTK dataset), best performances are systematically obtained with \mathcal{I}_{DA} . For example, with a mask length of 400 ms, \mathcal{I}_{EA} gets a PESQ score of 2.39, a STOI score of 0.79, and a CER of 19%, whereas \mathcal{I}_{DA} yields scores of 2.66, 0.83, and 18% respectively. The difference probably stems from the difficulty for \mathcal{I}_{EA} to compress in a single codebook all the inter-speaker variability. The use of a speaker embedding as done in \mathcal{I}_{DA} appears to be a much more efficient strategy.

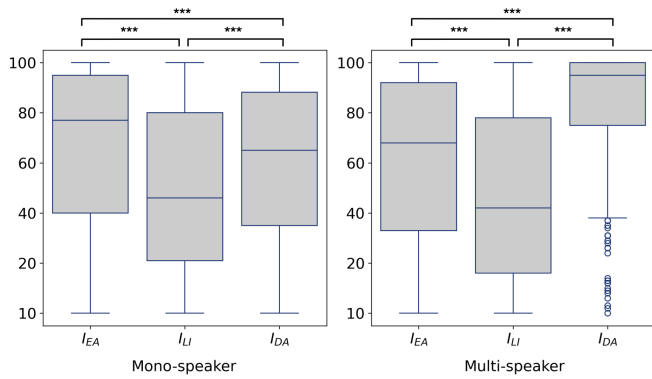


Fig. 3. Boxplots illustrating the distribution of the MUSHRA scores for the two models \mathcal{I}_{EA} and \mathcal{I}_{DA} , and for the \mathcal{I}_{LI} baseline (informed inpainting with a 200 ms-length mask). *** indicates that the differences between each pair of inpainting frameworks were found very significant (i.e. $p \leq 0.001$).

2) *Perceptual evaluation*: Results of the perceptual evaluation, conducted in the informed case with masks of 200 ms, are presented in Fig. 3. We assessed here the significance of the *framework* (\mathcal{I}_{LI} , \mathcal{I}_{DA} , \mathcal{I}_{EA}) factor with the participants as a random effect, and pairwise comparison displays significant differences between all frameworks. These results confirm all the trends revealed by the objective scores. Both proposed frameworks clearly outperform the baseline. The \mathcal{I}_{EA} framework provides better results than the \mathcal{I}_{DA} framework in the mono-speaker case, and the opposite is observed in the multi-speaker case (with an even more marked difference between the two frameworks). It is interesting to note that the performance levels obtained for the two proposed frameworks exceed 80%, and even 90% for the \mathcal{I}_{DA} framework in the multi-speaker case, for which the reconstructed signal is very close to the original signal.

C. Blind inpainting

The results of the objective evaluation of blind inpainting in terms of PESQ, STOI and CER scores are presented in Table II. To compare informed vs. blind inpainting, we assessed the significance of *mask length* (100, 200, 400 ms), *framework* (\mathcal{I}_{DA} , \mathcal{I}_{EA}), *dataset* (mono- and multi-speaker) and *type of inpainting* (informed vs. blind) with the test utterances as a random factor for each objective metric. Note that compared to Section IV-B1, the \mathcal{I}_{LI} level is removed from the *framework* factor, as it is not evaluated in the blind inpainting case. Statistical analysis shows that all factors and all their interactions have a significant effect on each objective metric.

a) *Informed vs. blind*: Pairwise comparisons show significant differences between the informed and blind metrics distributions, for each *framework*, *dataset*, and *mask length*. Compared to the informed inpainting configuration, the blind configuration is more challenging (the position of the mask is unknown and the full signal hence is reconstructed). As expected, it leads to lower performance, and this is observed for both \mathcal{I}_{EA} and \mathcal{I}_{DA} , for both datasets, all mask lengths, and all metrics. For example, for blind

inpainting with a 200 ms mask length in the mono-speaker case, \mathcal{I}_{EA} gets a STOI score of 0.84, compared to 0.93 in the corresponding informed case. Moreover, informed inpainting methods consistently exhibit lower CER, reflecting higher accuracy in reconstructing corrupted segments.

b) *Effect of mask length, framework, and dataset*: All pairs of distributions across the three factors are significant, except in terms of PESQ between mono- and multi-speaker datasets in the $\mathcal{I}_{DA} \times 200$ ms (\blacktriangleleft) condition ; in terms of STOI between the \mathcal{I}_{DA} and \mathcal{I}_{EA} frameworks in the 400 ms \times multi-speaker (\blacklozenge) condition and between mono- and multi-speaker in the $\mathcal{I}_{DA} \times 100$ ms (\blacktriangleup) and $\mathcal{I}_{DA} \times 400$ ms (\blacktriangleright) conditions. Interestingly, the interactions between the *type of inpainting* and each of these three factors are weak, as all the trends observed in the informed inpainting case remain in the blind inpainting case. Similarly to informed inpainting, performances of all metrics drop as mask length increase. Above all, the interaction between *framework* and *dataset* is still present, as the \mathcal{I}_{EA} framework provides better results than the \mathcal{I}_{DA} framework in the mono-speaker case, and the opposite is observed in the multi-speaker case.

D. Comparison with other studies

As announced in Section III-C, we compare the overall performance of the proposed frameworks with that of two recently published methods based on supervised deep learning [5], [6]. We recall that, since no source code was available for these techniques, we use the scores reported in the papers, and we compare the performances only in terms of order of magnitudes.

In [5], with a training and test on a multi-speaker dataset (LibriSpeech) and in the informed inpainting case, the authors reported a PESQ (resp. STOI) score of 3.24, 2.81, and 2.18 (resp. 0.94, 0.89, and 0.73) for mask lengths of 100, 200, and 400 ms, respectively. In [6], the authors reported PESQ (resp. STOI) scores of 3.30, 2.61, and 1.76 (resp. 0.96, 0.89, and 0.73) for similar masks and dataset. In our study, the best scores on the same settings for \mathcal{I}_{DA} (resp. \mathcal{I}_{EA}), were 3.13, 2.93, and 2.66 (resp. 3.06, 2.70, and 2.39) for PESQ, and 0.93, 0.88, and 0.83 (resp. 0.90, 0.85, and 0.79) for STOI (see Table I, multi-speaker).

For the blind case, we can only compare our results to those reported in [5] (Table 3, condition “FC-gaps”) since it is not treated in [6] (to the best of our understanding). In this case, our performances are significantly lower, both in terms of STOI and PESQ. For example, for a mask length of 400 ms [5] reported a quite high STOI score of 0.71 when we obtained only 0.52 with the (best) framework \mathcal{I}_{DA} . The differences between the two techniques are smaller when the mask length is shorter (e.g. a PESQ score of 2.72 in [5] for a mask length of 200 ms vs. 2.31 with \mathcal{I}_{DA}). Further experiments could be useful to better understand the origin of these differences in the case of blind inpainting. We would need to check that this is not simply due to the nature of the training/test datasets, to the analysis-synthesis ability of the methods, or to a different method of calculating the PESQ and STOI scores.

To conclude, this “meta-comparison” shows that the two proposed frameworks \mathcal{I}_{EA} and \mathcal{I}_{DA} seem to outperform other approaches based on supervised learning, at least in the informed case, and in particular for long masks (i.e., 400 ms). Here again, this can be explained by the ability of a powerful SSL model, pre-trained on a huge amount of data, to extract the high-level linguistic information (e.g., syntactic and semantic) of the sentence to be reconstructed, based on the contextual non-missing information.

V. CONCLUSION

This study evaluates the extent to which the pretext task of an unsupervised SSL model can be leveraged in an inpainting task. In particular, we investigate the ability of a non-causal SSL to “fill in the gap” by reconstructing a missing part of a speech signal from its surrounding context, and when combined with a neural vocoder (used as a decoder), to reconstruct the speech waveform. Two ways of combining non-causal prediction using a Transformer-based encoder and a neural vocoder were compared. Objective and perceptual evaluations showed that fine-tuning the SSL encoder for inpainting is the best strategy when dealing with mono-speaker data, while adapting the decoder performed better in the multi-speaker case. Further work will focus (i) on a fine-grained analysis of the inpainted speech at different linguistic scales (phonetic, syllabic, morphologic), and (ii) on the relationship between the context actually used by the SSL encoder on one hand, and the length and linguistic complexity of the signal to be reconstructed, on the other. Finally, in addition to their technological applications, the proposed speech inpainting systems, and SSL models in general, provide a means of finely quantifying the amount of predictable information in the speech signal. Therefore, they can be potentially useful for studying, through computational modelling and simulation, some of the predictive processes underlying speech perception [36], [37]. The proposed framework based on non-causal prediction could complement other studies conducted in the context of the predictive coding framework and focusing on causal predictions (e.g. [38], [39], [40]).

REFERENCES

- [1] C. Perkins, O. Hodson, and V. Hardman, “A survey of packet loss recovery techniques for streaming audio,” *IEEE Network*, vol. 12, no. 5, pp. 40–48, 1998.
- [2] G. Chantas, S. Nikolopoulos, and I. Kompatsiaris, “Sparse audio inpainting with variational Bayesian inference,” in *Proc. IEEE International Conference on Consumer Electronics (ICCE)*, Las Vegas, NV, January 12–14 2018, pp. 1–6.
- [3] M. Lagrange, S. Marchand, and J.-B. Rault, “Long interpolation of audio signals using linear prediction in sinusoidal modeling,” *Journal of the Audio Engineering Society*, vol. 53, no. 10, pp. 891–905, 2005.
- [4] A. Marafioti, P. Majdak, N. Holighaus, and N. Perraudin, “GACELA: A generative adversarial context encoder for long audio inpainting of music,” *IEEE Journal of Selected Topics in Signal Processing*, vol. 15, no. 1, pp. 120–131, 2021.
- [5] M. Kegler, P. Beckmann, and M. Cernak, “Deep speech inpainting of time-frequency masks,” in *Proc. of Interspeech*, Shanghai, China, October 25–29 2020, pp. 3276–3280.
- [6] H. Zhao, “A GAN speech inpainting model for audio editing software,” in *Proc. of Interspeech*, Dublin, Ireland, August 20–24 2023, pp. 5127–5131.
- [7] W. Etter, “Restoration of a discrete-time signal segment by interpolation based on the left-sided and right-sided autoregressive parameters,” *IEEE Transactions on Signal Processing*, vol. 44, no. 5, pp. 1124–1135, 1996.
- [8] N. Perraudin, N. Holighaus, P. Majdak, and P. Balazs, “Inpainting of long audio segments with similarity graphs,” *IEEE/ACM Transactions on Audio, Speech, and Language Processing*, vol. 26, no. 6, pp. 1079–1090, 2018.
- [9] A. Marafioti, N. Perraudin, N. Holighaus, and P. Majdak, “A context encoder for audio inpainting,” *IEEE/ACM Transactions on Audio, Speech, and Language Processing*, vol. 27, no. 12, pp. 2362–2372, 2019.
- [10] P. Beckmann, M. Kegler, H. Saltini, and M. Cernak, “Speechvgg: A deep feature extractor for speech processing,” *arXiv preprint arXiv:1910.09909*, 2019.
- [11] G. Morrone, D. Michelsanti, Z.-H. Tan, and J. Jensen, “Audio-visual speech inpainting with deep learning,” in *Proc. IEEE International Conference on Acoustics, Speech and Signal Processing (ICASSP)*, Toronto, ON, Canada, June 6–11 2021, pp. 6653–6657.
- [12] L. Bahrman, M. Krémé, P. Magron, and A. Deleforge, “Signal inpainting from Fourier magnitudes,” in *Proc. European Signal Processing Conference (EUSIPCO)*, Helsinki, Finland, September 4–8 2023, pp. 116–120.
- [13] J. Le Roux, H. Kameoka, N. Ono, and S. Sagayama, “Fast signal reconstruction from magnitude STFT spectrogram based on spectrogram consistency,” in *Proc. International Conference on Digital Audio Effects (DAFx)*, Graz, Austria, September 6–10 2010.
- [14] A. Mohamed, H.-y. Lee, L. Borgholt, J. D. Havtorn, J. Edin, C. Igel, K. Kirchhoff, S.-W. Li, K. Livescu, L. Maaløe, T. N. Sainath, and S. Watanabe, “Self-supervised speech representation learning: A review,” *IEEE Journal of Selected Topics in Signal Processing*, vol. 16, no. 6, pp. 1179–1210, 2022.
- [15] G.-P. Yang, S.-L. Yeh, Y.-A. Chung, J. Glass, and H. Tang, “Autoregressive predictive coding: A comprehensive study,” *IEEE Journal of Selected Topics in Signal Processing*, vol. 16, no. 6, pp. 1380–1390, 2022.
- [16] A. van den Oord, Y. Li, and O. Vinyals, “Representation learning with contrastive predictive coding,” 2018. [Online]. Available: <https://arxiv.org/abs/1807.03748>
- [17] W.-N. Hsu, B. Bolte, Y.-H. Tsai, K. Lakhotia, R. Salakhutdinov, and A. Mohamed, “HuBERT: Self-supervised speech representation learning by masked prediction of hidden units,” *IEEE/ACM Transactions on Audio, Speech, and Language Processing*, vol. 29, pp. 3451–3460, 2021.
- [18] A. Baevski, Y. Zhou, A. Mohamed, and M. Auli, “wav2vec 2.0: A framework for self-supervised learning of speech representations,” in *Advances in Neural Information Processing Systems*, vol. 33, Vancouver, Canada, December 6–12 2020, pp. 12 449–12 460.
- [19] S. Chen, C. Wang, Z. Chen, Y. Wu, S. Liu, Z. Chen, J. Li, N. Kanda, T. Yoshioka, X. Xiao, J. Wu, L. Zhou, S. Ren, Y. Qian, Y. Qian, J. Wu, M. Zeng, X. Yu, and F. Wei, “WavLM: Large-scale self-supervised pre-training for full stack speech processing,” *IEEE Journal of Selected Topics in Signal Processing*, vol. 16, no. 6, pp. 1505–1518, 2022.
- [20] A. Pasad, B. Shi, and K. Livescu, “Comparative layer-wise analysis of self-supervised speech models,” in *Proc. of IEEE International Conference on Acoustics, Speech and Signal Processing (ICASSP)*, Rhodes Island, Greece, June 4–10 2023, pp. 1–5.
- [21] S. wen Yang, P.-H. Chi, Y.-S. Chuang, C.-I. J. Lai, K. Lakhotia, Y. Y. Lin, A. T. Liu, J. Shi, X. Chang, G.-T. Lin, T.-H. Huang, W.-C. Tseng, K. tik Lee, D.-R. Liu, Z. Huang, S. Dong, S.-W. Li, S. Watanabe, A. Mohamed, and H. yi Lee, “SUPERB: Speech Processing Universal PERFORMANCE Benchmark,” in *Proc. of Interspeech*, Brno, Czechia, August 30 - September 3 2021, pp. 1194–1198.
- [22] A. van den Oord, S. Dieleman, H. Zen, K. Simonyan, O. Vinyals, A. Graves, N. Kalchbrenner, A. Senior, and K. Kavukcuoglu, “WaveNet: A Generative Model for Raw Audio,” in *Proc. ISCA Speech Synthesis Workshop*, Vienna, Austria, September 20–22 2019.
- [23] J. Kong, J. Kim, and J. Bae, “Hifi-gan: Generative adversarial networks for efficient and high fidelity speech synthesis,” *Advances in Neural Information Processing Systems*, vol. 33, pp. 17 022–17 033, December 6–12 2020.
- [24] A. Polyak, Y. Adi, J. Copet, E. Kharitonov, K. Lakhotia, W.-N. Hsu, A. Mohamed, and E. Dupoux, “Speech Resynthesis from Discrete Disentangled Self-Supervised Representations,” in *Proc. of Interspeech*, Brno, Czechia, August 30 - September 3 2021, pp. 3615–3619.
- [25] O. Perrotin, B. Stephenson, S. Gerber, and G. Bailly, “The Blizzard Challenge 2023,” in *Proc. Blizzard Challenge Workshop*, Grenoble, France, August 29 2023, pp. 1–27.
- [26] K. Ito and L. Johnson, “The LJ Speech Dataset,” <https://keithito.com/LJ-Speech-Dataset/>, 2017.

- [27] J. Yamagishi, C. Veaux, and K. MacDonald, “CSTR VCTK Corpus: English Multi-speaker Corpus for CSTR Voice Cloning Toolkit (version 0.92),” University of Edinburgh. The Centre for Speech Technology Research (CSTR), Tech. Rep., 2019.
- [28] J. Kahn, M. Rivière, W. Zheng, E. Kharitonov, Q. Xu, P. E. Mazaré, J. Karadayi, V. Liptchinsky, R. Collobert, C. Fuegen, T. Likhomanenko, G. Synnaeve, A. Joulin, A. Mohamed, and E. Dupoux, “Libri-Light: A benchmark for ASR with limited or no supervision,” in *Proc. IEEE International Conference on Acoustics, Speech and Signal Processing (ICASSP)*, Barcelona, Spain, May 4-8 2020, pp. 7669–7673, <https://github.com/facebookresearch/libri-light>.
- [29] G. Heigold, I. Moreno, S. Bengio, and N. Shazeer, “End-to-end text-dependent speaker verification,” in *Proc. or IEEE International Conference on Acoustics, Speech and Signal Processing (ICASSP)*, Shanghai, China, 2016, pp. 5115–5119.
- [30] D. P. Kingma and J. Ba, “Adam: A method for stochastic optimization,” in *International Conference on Learning Representations (ICLR)*, San Diego, CA, USA, May 7-9 2015.
- [31] A. W. Rix, J. G. Beerends, M. P. Hollier, and A. P. Hekstra, “Perceptual evaluation of speech quality (PESQ)-a new method for speech quality assessment of telephone networks and codecs,” in *Proc. of IEEE International Conference on Acoustics, Speech and Signal Processing (ICASSP)*, vol. 2, Salt Lake City, UT, USA, May 7-11 2001, pp. 749–752.
- [32] C. H. Taal, R. C. Hendriks, R. Heusdens, and J. Jensen, “A short-time objective intelligibility measure for time-frequency weighted noisy speech,” in *Proc. IEEE International Conference on Acoustics, Speech and Signal Processing (ICASSP)*, Dallas, TX, USA, March 14-19 2010, pp. 4214–4217.
- [33] A. Radford, J. W. Kim, T. Xu, G. Brockman, C. McLeavey, and I. Sutskever, “Robust speech recognition via large-scale weak supervision,” in *International Conference on Machine Learning*. Honolulu, Hawaii, USA: PMLR, July 23-29 2023, pp. 28 492–28 518.
- [34] N. Jillings, D. Moffat, B. De Man, and J. D. Reiss, “Web Audio Evaluation Tool: A browser-based listening test environment,” in *Proc. of the Sound and Music Computing Conference*, Maynooth, Ireland, July 26 - August 1 2015.
- [35] ITU, “Method for the subjective assessment of intermediate quality level of audio systems,” International Telecommunication Union, Tech. Rep. ITU-R BS.1534-3, October 2015. [Online]. Available: <https://www.itu.int/rec/R-REC-BS.1534>
- [36] K. Friston and S. Kiebel, “Predictive coding under the free-energy principle,” *Philosophical transactions of the Royal Society B: Biological sciences*, vol. 364, no. 1521, pp. 1211–1221, 2009.
- [37] A. Tavano and M. Scharinger, “Prediction in speech and language processing,” *Cortex*, vol. 68, pp. 1–7, 2015.
- [38] T. Hueber, E. Tatulli, L. Girin, and J.-L. Schwartz, “Evaluating the Potential Gain of Auditory and Audiovisual Speech-Predictive Coding Using Deep Learning,” *Neural Computation*, vol. 32, no. 3, pp. 596–625, 03 2020. [Online]. Available: https://doi.org/10.1162/neco_a_01264
- [39] C. Caucheteux, A. Gramfort, and J.-R. King, “Evidence of a predictive coding hierarchy in the human brain listening to speech,” *Nature human behaviour*, vol. 7, no. 3, pp. 430–441, 2023.
- [40] M. Heilbron, B. V. Ehinger, P. Hagoort, and F. P. de Lange, “Tracking naturalistic linguistic predictions with deep neural language models,” *2019 Conference on Cognitive Computational Neuroscience*, 2019. [Online]. Available: <https://api.semanticscholar.org/CorpusID:202542733>